jove

On-Chip Octanol-Assisted Liposome Assembly for Bioengineering

Chang Chen[*,1], **Ketan A. Ganar**[*,1], **Siddharth Deshpande**[1]

[1] Laboratory of Physical Chemistry and Soft Matter, Wageningen University & Research

[*] These authors contributed equally

Corresponding Author

Siddharth Deshpande
siddharth.deshpande@wur.nl

Citation

Chen, C., Ganar, K.A., Deshpande, S. On-Chip Octanol-Assisted Liposome Assembly for Bioengineering. *J. Vis. Exp.* (193), e65032, doi:10.3791/65032 (2023).

Date Published

March 17, 2023

DOI

10.3791/65032

URL

jove.com/video/65032

Abstract

Microfluidics is a widely used tool to generate droplets and vesicles of various kinds in a controlled and high-throughput manner. Liposomes are simplistic cellular mimics composed of an aqueous interior surrounded by a lipid bilayer; they are valuable in designing synthetic cells and understanding the fundamentals of biological cells in an *in vitro* fashion and are important for applied sciences, such as cargo delivery for therapeutic applications. This article describes a detailed working protocol for an on-chip microfluidic technique, octanol-assisted liposome assembly (OLA), to produce monodispersed, micron-sized, biocompatible liposomes. OLA functions similarly to bubble blowing, where an inner aqueous (IA) phase and a surrounding lipid-carrying 1-octanol phase are pinched off by surfactant-containing outer fluid streams. This readily generates double-emulsion droplets with protruding octanol pockets. As the lipid bilayer assembles at the droplet interface, the pocket spontaneously detaches to give rise to a unilamellar liposome that is ready for further manipulation and experimentation. OLA provides several advantages, such as steady liposome generation (>10 Hz), efficient encapsulation of biomaterials, and monodispersed liposome populations, and requires very small sample volumes (~50 µL), which can be crucial when working with precious biologicals. The study includes details on microfabrication, soft-lithography, and surface passivation, which are needed to establish OLA technology in the lab. A proof-of-principle synthetic biology application is also shown by inducing the formation of biomolecular condensates inside the liposomes *via* transmembrane proton flux. It is anticipated that this accompanying video protocol will facilitate the readers to establish and troubleshoot OLA in their labs.

Introduction

All cells have a plasma membrane as their physical boundary, and this membrane is essentially a scaffold in the form of a lipid bilayer formed by the self-assembly of amphiphilic lipid molecules. Liposomes are the minimal synthetic counterparts of biological cells; they have an aqueous lumen surrounded by phospholipids, which form a lipid bilayer with the hydrophilic head groups facing the aqueous phase and the hydrophobic tails buried inward. The stability of liposomes is governed by the hydrophobic effect, as well as the hydrophilicity between the polar groups, van der Waals forces between the hydrophobic carbon tails, and the hydrogen bonding between water molecules and the hydrophilic heads[1,2]. Depending on the number of lipid bilayers, liposomes can be classified into two main categories, namely, unilamellar vesicles comprising a single bilayer and multilamellar vesicles constructed from multiple bilayers. Unilamellar vesicles are further classified based on their sizes. Typically spherical in shape, they can be produced in a variety of sizes, including small unilamellar vesicles (SUV, 30-100 nm diameter), large unilamellar vesicles (LUV, 100-1,000 nm diameter), and finally, giant unilamellar vesicles (GUV, >1,000 nm diameter)[3,4]. Various techniques have been developed to produce liposomes, and these can be categorized broadly into bulk techniques[5] and microfluidic techniques[6]. Commonly practiced bulk techniques include lipid film rehydration, electroformation, inverted emulsion transfer, and extrusion[7,8,9,10]. These techniques are relatively simple and effective, and these are the prime reasons for their widespread usage in the synthetic biology community. However, at the same time, they suffer from major drawbacks with regard to the polydispersity in size, the lack of control over the lamellarity, and low encapsulation efficiency[7,11]. Techniques like continuous droplet interface crossing encapsulation (cDICE)[12] and droplet shooting and size filtration (DSSF)[13] overcome these limitations to some extent.

Microfluidic approaches have been rising to prominence over the last decade. Microfluidic technology provides a controllable environment for manipulating fluid flows within user-defined microchannels owing to the characteristic laminar flow and diffusion-dominated mass transfer. The resulting lab-on-a-chip devices offer unique possibilities for the spatiotemporal control of molecules, with significantly reduced sample volumes and multiplexing capabilities[14]. Numerous microfluidic methods to make liposomes have been developed, including pulsed jetting[15], double emulsion templating[16], transient membrane ejection[17], droplet emulsion transfer[18], and hydrodynamic focusing[19]. These techniques produce monodispersed, unilamellar, cell-sized liposomes with high encapsulation efficiency and high throughput.

This article details the procedure for octanol-assisted liposome assembly (OLA), an on-chip microfluidic method based on the hydrodynamic pinch-off and subsequent solvent dewetting mechanism[20] (**Figure 1**). One can relate the working of OLA to a bubble-blowing process. A six-way junction focuses the inner aqueous (IA) phase, two lipid-carrying organic (LO) streams, and two surfactant-containing outer aqueous (OA) streams at a single spot. This results in water-in-(lipids + octanol)-in-water double emulsion droplets. As these droplets flow downstream, interfacial energy minimization, external shear flow, and interaction with the channel walls lead to the formation of a lipid

bilayer at the interface as the solvent pocket becomes detached, thus forming unilamellar liposomes. Depending on the size of the octanol pocket, the dewetting process can take tens of seconds to a couple of minutes. At the end of the exit channel, the less dense octanol droplets float to the surface, whereas the heavier liposomes (due to a denser encapsulated solution) sink to the bottom of the visualization chamber ready for experimentation. As a representative experiment, the process of liquid-liquid phase separation (LLPS) inside liposomes is demonstrated. For that, the required components are encapsulated inside liposomes at an acidic pH that prevents LLPS. By externally triggering a pH change and, thus, a transmembrane proton flux, phase-separated condensate droplets are formed inside the liposomes. This highlights the effective encapsulation and manipulation capabilities of the OLA system.

Protocol

1. Fabricating the master wafer

1. Take a 4 in (10 cm) diameter clean silicon wafer (see **Table of Materials**). Clean it further using pressurized air to remove any dust particles.
2. Mount the wafer on a spin coater, and gently dispense ~5 mL of a negative photoresist (see **Table of Materials**) in the center of the wafer. Try to avoid air bubbles, as they might interfere with the downstream printing process of the wafer.
3. To obtain a 10 µm thick photoresist layer, spin-coat the wafer at 500 rpm for 30 s with an acceleration of 100 rpm/s for initial spreading, followed by a 60 s spin at 3,000 rpm with an acceleration of 500 rpm/s. In case a different thickness is desired, change the spinning parameters according to the manufacturer's instructions.
4. Bake the wafer on a heating plate for 2 min at 65 °C and then for 5 min at 95 °C.
5. Once the wafer cools down, mount the wafer in the printing chamber of the direct-write optical lithography machine (see **Table of Materials**), and feed the OLA design (**Figure 2A**, **Supplementary Coding File 1**) into the software.
   NOTE: The OLA design essentially consists of two OA channels, two LO channels, and one IA channel, which merge to form a six-way junction that continues as a post-production channel and ends up in the experimental well (EW).
6. Print the OLA design(s) on the coated wafer using a UV laser (see **Table of Materials**) with a dose of 300 mJ/cm^2.
7. Once the design is printed, bake the wafer at 65 °C for 1 min, followed by 95 °C for 3 min.
8. At this point, ensure that the outline of the printed device appears on the wafer and is visible to the naked eye. To wash off the uncured photoresist, dip the wafer in a glass beaker containing the developer solution (see **Table of Materials**) until the uncured photoresist is fully removed.
   NOTE: Excess developer treatment can affect the design resolution.
9. Wash the wafer with acetone, isopropanol, and deionized (DI) water in sequence, and finally, with pressurized air/N_2 using a blow gun.
10. Hard-bake the wafer at 150 °C for 30 min to ensure that the printed design is firmly attached to the wafer surface and does not come off in the downstream fabrication process. The master wafer is then ready for further use (**Figure 2B**).

2. Preparing the microfluidic device

1. Place the master wafer on a square piece of aluminum, and wrap the aluminum foil around the wafer, forming a well-like structure (**Figure 2C**).
2. Measure 40 g of polydimethylsiloxane (PDMS) and 4 g of curing agent (10:1, weight ratio, see **Table of Materials**) in a 50 mL centrifuge tube, and mix vigorously using a spatula or a pipette tip for 2-3 min.
3. The vigorous mixing of the PDMS and curing agent traps air bubbles inside the mixture. Spin the tube at 100 x *g* for 2-3 min to remove majority of large air bubbles.
4. Pour approximately 15-20 g of the mixture prepared in step 2.3 over the master wafer, and de-gas using a desiccator. Save the excess mixture to make PDMS-coated glass slides (step 3).
5. Incubate the assembly in an oven at 70 °C for at least 2 h.
6. Take the master wafer out of the oven and let it cool down. To remove the solidified PDMS block, remove the aluminum foil, and carefully peel off the PDMS block from the edge of the wafer.
   NOTE: The wafer is fragile and might break, so it is important to do this process carefully.
7. Once the PDMS block is removed, keep the patterned structure facing upward, and using a sharp blade or a scalpel, cut individual PDMS blocks, each containing a single microfluidic device.
8. Place the PDMS block on a dark surface, and adjust the light direction (a table lamp comes in handy for this) so that the engraved channels are shiny and, as a result, visible. Make holes in the inlets and the exit channel using biopsy punches of 0.5 mm and 3 mm diameter (see **Table of Materials**), respectively.
   NOTE: Use a sharp biopsy punch to avoid cracks in the PDMS, which can cause leakage later. Gently push the biopsy punch through the PDMS block, and ensure it passes completely through it. To remove the biopsy punch, gently retract it while rotating it in alternate directions. The PDMS block with the engraved OLA design is now ready to bind to a PDMS-coated glass slide.

3. Making the PDMS-coated glass slide

1. Take a transparent glass coverslip, pour approximately 0.5 mL of PDMS (prepared in excess in step 2.4) onto the center of the glass slide, and spread it across the coverslip by gently tilting the glass slide, ensuring total coverage of the glass slide with PDMS.
2. Mount the glass slide on the spin coater, ensure its centrally placed (so that the middle of the slide overlaps with the center of the pressure shaft), and spin the glass slide at 500 rpm for 15 s (at an increment of 100 rpm/s) and then at 1,000 rpm for 30 s (at an increment of 500 rpm/s).
3. Place the PDMS-coated glass slide (coated side facing upward) on a raised platform like a block of PDMS (1 cm x 1 cm) in a covered Petri dish, and bake it at 70 °C for 2 h.

4. Bonding of the microfluidic device

1. Clean the PDMS block (prepared in step 2) by sticking and removing commercially available scotch tape (see **Table of Materials**) twice. Ensure to keep the cleaned side facing up until use.
2. Clean the PDMS-coated glass slide with pressurized air/ N_2 using a blow gun, and keep the clean side facing up.

3. Place the PDMS block (engraved channels facing up) and the PDMS-coated glass slide (coated side facing up) in the vacuum chamber of the plasma cleaner (see **Table of Materials**).
4. Switch on the vacuum, and expose the contents to air plasma at a radio frequency of 12 MHz (RF mode high) for 15 s to activate the surfaces. Oxygen plasma can be seen in the form of a pinkish hue.
5. Immediately after the plasma treatment, place the PDMS-coated glass slide on a clean surface with the PDMS side facing upward. Gently place the PDMS block with the microfluidic pattern now facing toward the PDMS-coated glass slide, allowing them to bond (**Figure 2D**).
   NOTE: Removing the air trapped in the device is crucial to ensure thorough bonding.
6. Bake the bonded devices at 70 °C for 2 h.

5. Surface functionalization of the microfluidic device

NOTE: Prior to surface functionalization, it is important to calibrate the pressure pump as per the manufacturer's protocol (see **Table of Materials**) and assemble the tubing to connect it to the microfluidic device.

1. Connecting the microfluidic device to the pressure pumps
   1. Connect the pressure-driven flow controller to an external pressure source (up to 6 bars). At least four independent air pressure channels are required: three individual modules of 0-2 bar, and one module of −0.9-4 bar.
   2. Calibrate the pressure pump according to the manufacturer's protocol (see **Table of Materials**).
   3. Cut the tubing (1/16 in OD x 0.02 in ID) into four equal-sized pieces approximately 20 cm in length.
   4. Insert 23 G stainless steel 90° bent connectors (see **Table of Materials**) at one end of each piece. This end is later inserted into the three inlets (OA, LO, and IA) of the microfluidic device and the fourth one is used to remove excess solution (step 5.2.5).
   5. Insert the other end of the tubing into the microfluidic reservoir stand, and seal it using microfluidic fittings, ensuring the tubing is long enough to touch the bottom of the reservoir (1.5 mL tubes, see **Table of Materials**). This prevents unwanted air bubbles from entering the microfluidic device during the PVA treatment/liposome production.
2. PVA treatment of the exit channel
   NOTE: Prior to liposome generation, it is crucial to render the device partially hydrophilic downstream of the production junction. This is done by treating these channels with 5% (w/v) polyvinyl alcohol (PVA) solution. The PVA solution is prepared by dissolving the PVA powder (see **Table of Materials**) in water at 80 °C for 3 h with constant stirring using a magnetic stirrer. Filter the solution prior to using it for surface treatment. Immediately after the bonding of the device, the microfluidic channels are hydrophilic due to the plasma-induced surface activation, and they will gradually become hydrophobic again. It is recommended to wait for 2 h after the baking (step 4.6) before starting the PVA treatment.
   1. Dispense 200 µL of 5% w/v PVA solution into a 1.5 mL tube, and connect it to the microfluidic reservoir stand. Insert the tubing (the one mentioned in step 5.1.3) such that one end is submerged in the PVA

solution and the other end is connected to the inlet of the OA channel of the microfluidic device.

NOTE: A lower PVA concentration can lead to sub-standard surface functionalization.

2. Repeat the above step without PVA (empty 1.5 mL tube), and connect it to the LO and IA channels.

3. Increase the pressure of the OA phase to 100 mbar to flow the PVA solution in the OA channels. Increase the pressures of the IA and LO phases to 120 mbar in order to prevent the backflow of PVA solution inside these channels (**Figure 2E**).

NOTE: If needed, adjust the pressures of the individual channels in order to keep the meniscus steady at the production junction.

4. Flow the PVA solution in this manner for approximately 5 min, ensuring complete functionalization of the exit channel.

5. To remove the PVA solution, detach the tubing from the OA inlet, and immediately increase the pressure in the LO and IA channels to 2 bar. Simultaneously, use a tubing connected to a negative pressure channel (−900 mbar) remove excess PVA first from the exit channel and then from the OA inlet (**Figure 2F**).

6. Bake the device at 120 °C for 15 min, and let it cool down before use. The device can be stored under ambient conditions for at least 1 month.

NOTE: It is recommended to wait for 1 day (at room temperature) before proceeding with OLA to ensure the untreated PDMS regains its hydrophobicity after the plasma treatment.

6. Octanol-assisted liposome assembly (OLA)

1. Preparing the lipid stock

NOTE: Here, a mixture of 1,2-dioleoyl-sn-glycero-3-phosphocholine (DOPC) and 1,2-dioleoyl-sn-glycero-3-phosphoethanolamine-N-(lissamine rhodamine B sulfonyl) (Liss Rhod PE) lipids (see **Table of Materials**) are used as an example; users should prepare the lipid composition they need in a similar manner.

1. Dispense 76 µL of DOPC (25 mg/mL) and 16.6 µL of Liss Rhod PE (1 mg/mL) into a round-bottom flask using separate glass syringes.

2. Keep the round-bottom flask upright, and use a compressed N_2 blow gun to give a gentle stream of nitrogen to evaporate the chloroform and form a dried lipid film at the bottom of the flask.

3. Place the flask in the desiccator for at least 2 h under a continuous vacuum to remove any remaining chloroform.

4. Add 100 µL of ethanol into the round-bottom flask, followed by gentle pipetting or shaking to ensure the lipids are dissolved to form a 10% (w/v) lipid stock.

NOTE: In case a particular lipid composition is not completely soluble in ethanol, use an ethanol/chloroform mixture, keeping the volume of chloroform as small as possible.

5. Pipette the solution into a dark glass vial. Gently flush the vial with nitrogen using a blow gun to replace the air with an inert atmosphere. Seal the lid with paraffin film, and store at −20 °C.

NOTE: The stock solution can be used for up to a few months. Each time the vial is opened, gently replace

the air with nitrogen, and reseal with lid with paraffin film.

2. Preparing the OLA solutions

    1. Make stock solutions of the indispensable components: 20 mM dextran (Mw 6,000); 60% (v/v) glycerol; a buffer of choice. In this case, 5x phosphate-buffered saline (0.68 M NaCl, 13.5 mM KCl, 50 mM Na_2HPO_4, 9 mM KH_2PO_4; pH 7.4) was prepared (see **Table of Materials**).

        NOTE: As pure glycerol is highly viscous, it is recommended to cut out a small piece at the end of the pipette tip in a slanted manner for effective pipetting.

    2. Prepare 100 µL of IA, OA, and exit solution (ES, the desired solution to fill the EW) samples. For ease of visualization, yellow fluorescent protein (YFP) was added to the IA solution in this particular case. Check the osmotic balance between the IA and OA by calculating the osmolarity of the encapsulated components and adding an appropriate amount of sugar or salt into the OA if needed. This is done in order to prevent the bursting or shrinking of the liposomes during production.

        NOTE: The final compositions of the three phases are as follows:

        IA: 15% glycerol, 5 mM dextran (Mw 6,000), 5.4 µM YFP, 1x PBS

        OA: 15% glycerol, 5% F68 surfactant, 1x PBS

        ES: 15% glycerol, 1x PBS

        A lower concentration of F68 surfactant negatively affects the generation of double emulsions.

    3. Prepare 80 µL of the LO phase by pipetting 4 µL of stock lipid into 76 µL of 1-octanol (see **Table of Materials**). The final concentration of DOPC is 5 mg/mL.

    4. Centrifuge the samples at 700 x *g* for 60 s to remove any large aggregates before proceeding with the microfluidic experiments. This prevents any obvious clogging factors from entering the microfluidic chip.

3. Liposome production

    1. Dispense the solutions (IA, LO, OA) into three 1.5 mL tubes, assemble them (as mentioned in step 5.1), and connect them to the PVA-treated microfluidic chip (step 5.2.6).

    2. Apply a positive pressure on the three channels: ~100 mbar on the IA and LO channels and ~200 mbar on the OA channel.

        NOTE: Since the OA pressure is higher than the others, the OA solution will be the first to arrive at EW; this is highly recommended.

    3. Once the OA solution reaches EW, decrease the OA pressure to 100 mbar and increase the LO to 200 mbar. The LO solution arriving at the production junction will likely result in air bubbles because of air being displaced from the LO channels. Once the air bubbles are dispensed into the EW, adjust the LO pressure to 100 mbar. Lastly, increase the IA pressure to 200 mbar, and wait until all the air in the IA channel is removed. The ideal sequence of arrival at the junction of the three phases is, thus, OA, LO, and IA.

    4. After removing the air from the three channels, adjust all the channel pressures to 50 mbar and pipette 10 µL of ES into the exit chamber. After pipetting the ES, put a cover slide on the exit hole to avoid evaporation. In case the LO is pushed

back, gradually increase the LO pressure in 1 mbar increments until it starts to flow to the junction.

5. Once all three phases start co-flowing at the junction, ensure double emulsion production begins, and adjust according to its quality (**Figure 3A-C**). Change the pressures gradually (steps of 0.1-1 mbar) rather than abruptly unless the pressure is being changed to eliminate an unwanted clog in the channel.

   NOTE: The channels to adjust depends on what is happening at the junction. For example, the IA needs to be decreased if the emulsions are too big; the OA needs to be increased if double emulsions form but burst instead of getting pinched off; and the LO needs to be decreased if the octanol pocket is too big.

6. Check that the double-emulsion droplets flow downstream to EW. As they flow, octanol pockets become more and more prominent and finally get pinched off, forming liposomes (**Figure 3D-F**). Ensure that the post-production channel is long enough and that the migration of the double emulsions is slow enough for dewetting.

   NOTE: Within minutes after decent production, liposomes and octanol droplets will exit the post-production channel and go into the EW. As a result, being less dense than water, the octanol droplets float to the surface of the ES. Due to the addition of dextran in the IA, the liposomes are heavier than their surroundings and go to the bottom of the chamber ready for observation and further manipulation.

Representative Results

This study demonstrates the formation of membraneless condensates *via* the process of liquid-liquid phase separation (LLPS) inside liposomes as a representative experiment.

Sample preparation

The IA, OA, ES, and feed solution (FS) are prepared as follows:

IA: 12% glycerol, 5 mM dextran, 150 mM KCl, 5 mg/mL poly-L-lysine (PLL), 0.05 mg/mL poly-L-lysine-FITC labeled (PLL-FITC), 8 mM adenosine triphosphate (ATP), 15 mM citrate-HCl (pH 4)

OA: 12% v/v glycerol, 5% w/v F68, 150 mM KCl, 15 mM citrate-HCl (pH 4)

ES: 12% glycerol, 150 mM KCl, 15 mM citrate-HCl (pH 4)

FS: 12% glycerol, 150 mM KCl, 75 mM Tris-HCl (pH 9)

Condensate formation inside liposomes

A simple assay of pH-sensitive complex coacervation of positively charged poly-L-lysine (PLL) and negatively charged multivalent adenosine triphosphate (ATP) was selected to demonstrate the phenomena of LLPS in liposomes. To prevent phase separation of polylysine and ATP during encapsulation, the pH of the solution was maintained at 4, at which ATP is neutral. Increasing the pH of the ES by adding FS (a buffer of pH 9) eventually increased the pH inside the liposomes due to transmembrane proton flux, making ATP negatively charged and triggering its phase separation with positively charged PLL[21] (**Figure 4A**). After about 2 h of liposome generation, the IA and LO pressures were switched off. The OA channel pressure was kept at 100 mbar to flow the remaining liposomes into the observation

chamber slowly. Once all the liposomes in the channel were recovered in the EW, the pressures were switched off to stop the flow and prevent the liposomes from moving. The liposomes generated at a lower pH showed a homogeneous fluorescence (from the encapsulated fluorescent PLL-FITC) in their lumen (**Figure 4B**,**D**). Octanol droplets floating at the surface were removed by carefully pipetting out 5 µL of solution from the top to prevent them from affecting further pipetting steps. Subsequently, 10 µL of FS buffer was added to the EW, which induced phase separation of the encapsulated PLL and ATP. The homogeneous FITC fluorescence from each liposome gradually transformed into distinct fluorescent condensate droplets. Eventually, the individual droplets merged into one bigger condensate droplet that freely diffused within the liposomes (**Figure 4C**,**E-G**).

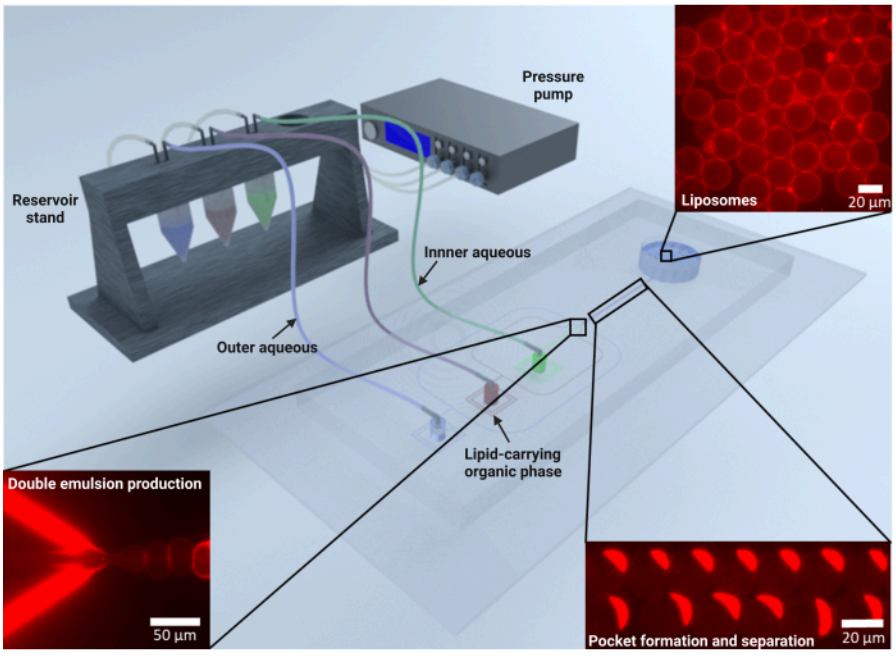

Figure 1: Schematic showing the assembly and working of OLA. The pressure controller is connected to the reservoirs containing outer aqueous, lipid-in-octanol, and inner aqueous solutions. The tubes inserted into the reservoirs are connected to the respective inlets of the OLA device. Appropriate flows in the three channels lead to the formation of water-in-(lipid-in-octanol)-in-water double emulsions. The formed double emulsions migrate to the exit well, during which the octanol pockets detach to form liposomes. The formed liposomes are collected at the bottom of the well for visualization and further experimentation. Please click here to view a larger version of this figure.

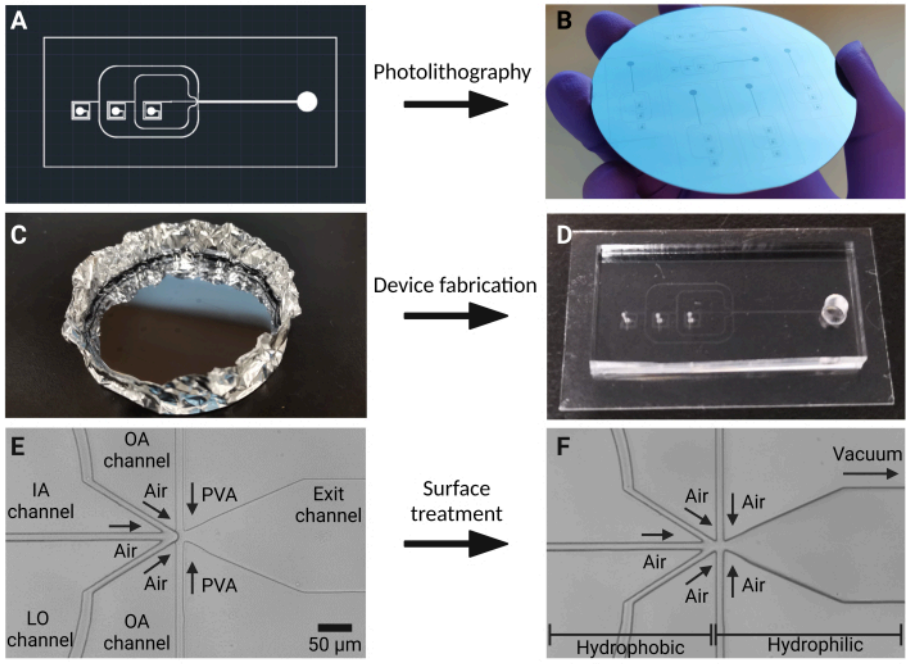

Figure 2: Preparation of the OLA chip (photolithography, microfabrication, surface treatment). (**A**) Digital design showing the key features of the OLA design, including three inlets, an outlet, and a six-way production junction. (**B**) A schematic of the master wafer showing multiple OLA designs produced using UV lithography. (**C**) A PDMS elastomer cast on the master wafer, placed in a well created out of aluminum foil, and cured by baking at 70 °C for 2 h. (**D**) A microfluidic device bonded using oxygen plasma treatment, where the PDMS block containing the OLA design is attached to a PDMS-coated glass slide. (**E**) Surface functionalization of the fabricated chip to make the device partially hydrophilic. This is done by flowing 5% w/v PVA for 5 min from the outer aqueous channel toward the exit channel. Positive air pressure in the other channels prevents the PVA solution from entering these channels. (**F**) PVA is removed by applying a vacuum in the exit channel. The device is baked at 120 °C for 15 min and is then ready to use. Please click here to view a larger version of this figure.

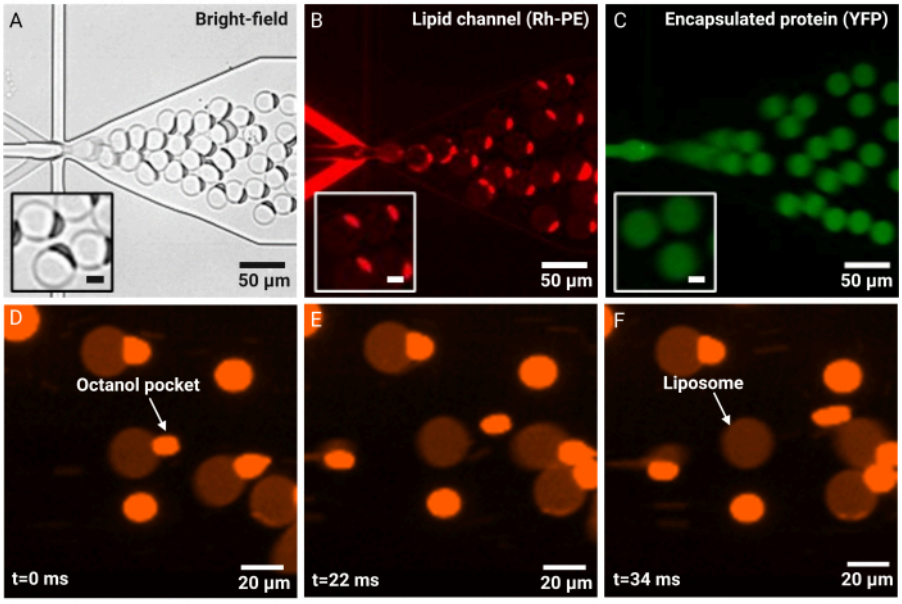

Figure 3: Demonstration of OLA efficiently producing monodispersed double emulsions and eventually liposomes with excellent encapsulation. (**A**) A bright-field image showing rapid generation of double-emulsion droplets. (**B**) The fluorescent lipid channel shows the formation of an octanol pocket due to partial dewetting. The lipid-in-octanol phase contained a mixture of DOPC (5 mg/mL) and Lis Rhod PE at a 1,000:1 ratio. (**C**) The inner aqueous channel showing encapsulation of yellow fluorescent protein (YFP). The insets in (**A-C**) show representative zoomed-in views of the respective panels (scale bars = 10 µm). (**D-F**) Dewetting of the octanol pocket in the exit channel, which forms a liposome. Please click here to view a larger version of this figure.

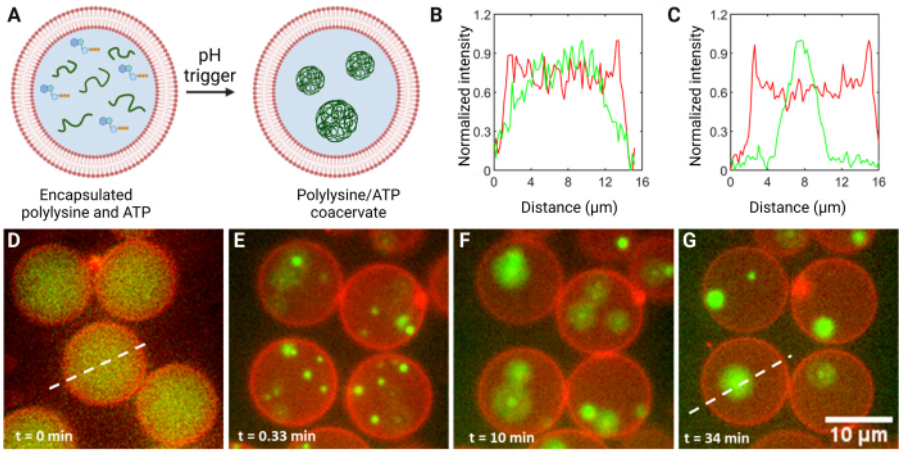

Figure 4: pH-triggered liquid-liquid phase separation of pLL/ATP within liposomes. (**A**) Schematic of the pH-dependent transitioning of the homogenous solution of pLL and ATP encapsulated within the liposome (left) to phase-separated pLL/ATP coacervates (right). The initial acidic environment in the liposome renders the molecular charge of ATP to be neutral, inhibiting coacervation. When the pH inside the liposomes equilibrates with the externally applied pH increase, ATP gains a negative charge, triggering coacervation. (**B-C**) Line graphs (corresponding to the dotted lines in panels [**D**] and [**G**], respectively) showing the spatial distribution of pLL (green channel) and the membrane (red channel). (**D-G**) Time-lapse images showing the formation of pLL/ATP coacervates within the liposomes. The external addition of a basic buffer raises the pH level inside the liposomes over the course of minutes and initiates coacervation. t = 0 min refers to the time just before the occurrence of the first coacervation event. Please click here to view a larger version of this figure.

Supplementary Coding File 1: CAD file of the OLA design. Please click here to download this File.

Discussion

Cellular complexity makes it extremely difficult to understand living cells when studied as a whole. Reducing the redundancy and interconnectivity of cells by reconstituting the key components in vitro is necessary to further our understanding of biological systems and create artificial cellular mimics for biotechnological applications[22,23,24]. Liposomes serve as an excellent minimal system to understand cellular phenomena. A non-exhaustive list of these phenomena includes cytoskeleton dynamics and resulting membrane deformations[25,26], spatiotemporal regulation of biomolecular condensates[27,28] and their interaction with the membrane[29], encapsulation of a wide variety of biomolecules, including cell-free transcription-translation systems[30], cell-free lipid synthesis[31], and evolution of proteins[32,33,34]. Liposomes have also been widely used as carriers for drug delivery and have been approved by the Food and Drug Administration (FDA) and European Medicines Agency (EMA) for clinical usage[11]. Liposomes and lipid-based nanoparticles are used as carriers for drug delivery, including mRNA vaccines like the recent COVID-19 vaccine[35].

This study describes a detailed protocol on photolithography, microfluidic assembly, and surface functionalization to perform the OLA technique in order to generate on-chip liposomes (**Figure 1** and **Figure 3**). The liposomes produced using OLA are monodispersed (coefficient of variation: 4%-11% of the mean) and in the biological cell-sized range (typically between 5-50 µm in diameter), and they can be tuned using appropriate flow velocities of the inner and outer aqueous channels[36]. For example, the liposome population seen in **Figure 1** has a size distribution of 23.3 µm ± 1.8 µm (*n* = 50). With typical production rates of 10-30 Hz, the formed liposomes are unilamellar, as was previously confirmed by inserting a single bilayer-specific transmembrane protein, alpha-hemolysin[36], into the membrane, as well as by using the dithionate-bleaching assay[37]. OLA is also compatible with a wide variety of lipid compositions, offering the user flexibility in the choice of lipids. Importantly, the initially used lipid composition is reflected in the final liposome composition[38].

Being a relatively new technology, there is further scope for improving OLA. For instance, surface functionalization using PVA is crucial but tedious to perform. An easier and simpler way to surface-functionalize the device would significantly reduce the chip fabrication time as well as chip-to-chip variability. Pluronic F68 surfactant is an important component in the outer aqueous phase to initially stabilize the double emulsions; nonetheless, its usage can be restrictive in certain cases. Replacing Pluronic F68 with a more biocompatible surfactant or complete surfactant removal may improve the versatility of the system. During the migration of generated double emulsions in the exit channel, they can burst due to shear. Upgrading the OLA design to improve the double emulsion stability and octanol pocket separation could, thus, increase the throughput. Nonetheless, OLA has several advantages, which mainly include the efficient encapsulation, monodispersed and unilamellar liposomes, and controlled on-chip experimentation.

OLA has been employed and adapted in a diverse range of studies, including growth and division of liposomes[39], studying the process of liquid-liquid phase separation[27] and its interaction with the membrane[21], and understanding bacterial growth bioproduct formation in liposomes[40]. OLA-based high-throughput assays are also being used to understand ion transport across the membrane[41] and drug permeability across the lipid bilayer[37], as a drug delivery system for therapeutic purposes[42], to study the effect of antimicrobials on membrane[43], and as a tool to encapsulate liquid crystals[44]. In addition to the wide range of applications of OLA technology, modified versions of OLA suited for particular purposes are being developed[45,46,47,48,49,50]. Overall, considering the pros and cons, we strongly believe that OLA is a versatile platform for synthetic biology.

Disclosures

The authors declare no conflicts of interest.

Acknowledgments

We would like to acknowledge Dolf Weijers, Vera Gorelova, and Mark Roosjen for kindly providing us with YFP. S.D. acknowledges financial support from the Dutch Research Council (grant number: OCENW.KLEIN.465).

References

1. Frezard, F. Liposomes: From biophysics to the design of peptide vaccines. *Brazilian Journal of Medical and Biological Research.* **32** (2), 181-189 (1999).
2. Monteiro, N., Martins, A., Reis, R. L., Neves, N. M. Liposomes in tissue engineering and regenerative

medicine. *Journal of the Royal Society Interface.* **11** (101), 20140459 (2014).

3. Mishra, H., Chauhan, V., Kumar, K., Teotia, D. A comprehensive review on liposomes: A novel drug delivery system. *Journal of Drug Delivery and Therapeutics.* **8** (6), 400-404 (2018).
4. Liu, W. et al. Research progress on liposomes: Application in food, digestion behavior and absorption mechanism. *Trends in Food Science & Technology.* **104**, 177-189 (2020).
5. Kamiya, K., Takeuchi, S. Giant liposome formation toward the synthesis of well-defined artificial cells. *Journal of Materials Chemistry B.* **5** (30), 5911-5923 (2017).
6. van Swaay, D., DeMello, A. Microfluidic methods for forming liposomes. *Lab on a Chip.* **13** (5), 752-767 (2013).
7. Lombardo, D., Kiselev, M. A. Methods of liposomes preparation: Formation and control factors of versatile nanocarriers for biomedical and nanomedicine application. *Pharmaceutics.* **14** (3), 543 (2022).
8. Zhang, H.Thin-film hydration followed by extrusion method for liposome preparation. In *Liposomes: Methods and Protocols.*, edited by D'Souza, G. G. M., 17-22. Humana. New York, NY (2017).
9. Filipczak, N., Pan, J., Yalamarty, S. S. K., Torchilin, V. P. Recent advancements in liposome technology. *Advanced Drug Delivery Reviews.* **156**, 4-22 (2020).
10. Has, C., Sunthar, P. A comprehensive review on recent preparation techniques of liposomes. *Journal of Liposome Research.* **30** (4), 336-365 (2020).
11. Large, D. E., Abdelmessih, R. G., Fink, E. A., Auguste, D. T. Liposome composition in drug delivery design, synthesis, characterization, and clinical application. *Advanced Drug Delivery Reviews.* **176**, 113851 (2021).
12. Abkarian, M., Loiseau, E., Massiera, G. Continuous droplet interface crossing encapsulation (cDICE) for high throughput monodisperse vesicle design. *Soft Matter.* **7** (10), 4610-4614 (2011).
13. Morita, M. et al. Droplet-shooting and size-filtration (DSSF) method for synthesis of cell-sized liposomes with controlled lipid compositions. *ChemBioChem.* **16** (14), 2029-2035 (2015).
14. Convery, N., Gadegaard, N. 30 years of microfluidics. *Micro and Nano Engineering.* **2**, 76-91 (2019).
15. Stachowiak, J. C. et al. Unilamellar vesicle formation and encapsulation by microfluidic jetting. *Proceedings of the National Academy of Sciences of the United States of America.* **105** (12), 4697-4702 (2008).
16. Chu, L. Y., Utada, A. S., Shah, R. K., Kim, J. W., Weitz, D. A. Controllable monodisperse multiple emulsions. *Angewandte Chemie.* **119** (47), 9128-9132 (2007).
17. Pautot, S., Frisken, B. J., Weitz, D. Engineering asymmetric vesicles. *Proceedings of the National Academy of Sciences of the United States of America.* **100** (19), 10718-10721 (2003).
18. Ota, S., Yoshizawa, S., Takeuchi, S. Microfluidic formation of monodisperse, cell-sized, and unilamellar vesicles. *Angewandte Chemie International Edition.* **48** (35), 6533-6537 (2009).
19. Carugo, D., Bottaro, E., Owen, J., Stride, E., Nastruzzi, C. Liposome production by microfluidics: Potential and limiting factors. *Scientific Reports.* **6**, 25876 (2016).

20. Deshpande, S., Dekker, C. On-chip microfluidic production of cell-sized liposomes. *Nature Protocols.* **13** (5), 856-874 (2018).
21. Last, M. G., Deshpande, S., Dekker, C. pH-controlled coacervate-membrane interactions within liposomes. *ACS Nano.* **14** (4), 4487-4498 (2020).
22. Jia, H. Schwille, P. Bottom-up synthetic biology: reconstitution in space and time. *Current Opinion in Biotechnology.* **60**, 179-187 (2019).
23. Ganar, K.A, Leijten, L., Deshpande, S. Actinosomes: Condensate-Templated Containers for Engineering Synthetic Cells. *ACE Synthetic Biology.* **11** (8), 2869-2879 (2022).
24. Gaut, N.T., Adamala, K. P. Reconstituting Natural Cell Elements in Synthetic Cells. *Advanced Biology.* **5** (3), 2000188 (2021).
25. Ganar, K. A., Honaker, L. W., Deshpande, S. Shaping synthetic cells through cytoskeleton-condensate-membrane interactions. *Current Opinion in Colloid & Interface Science.* **54**, 101459 (2021).
26. Bashirzadeh, Y., Liu, A. P. Encapsulation of the cytoskeleton: Towards mimicking the mechanics of a cell. *Soft Matter.* **15** (42), 8425-8436 (2019).
27. Deshpande, S. et al. Spatiotemporal control of coacervate formation within liposomes. *Nature Communications.* **10**, 1800 (2019).
28. Love, C. et al. Reversible pH-responsive coacervate formation in lipid vesicles activates dormant enzymatic reactions. *Angewandte Chemie.* **132** (15), 6006-6013 (2020).
29. Lu, T. et al. Endocytosis of coacervates into liposomes. *Journal of the American Chemical Society.* **144** (30), 13451-13455 (2022).
30. Van de Cauter, L. et al. Optimized cDICE for efficient reconstitution of biological systems in giant unilamellar vesicles. *ACS Synthetic Biology.* **10** (7), 1690-1702 (2021).
31. Blanken, D., Foschepoth, D., Serrão, A. C., Danelon, C. Genetically controlled membrane synthesis in liposomes. *Nature Communications.* **11**, 4317 (2020).
32. Bouzetos, E., Ganar, K. A., Mastrobattista, E., Deshpande, S., van der Oost, J. (R) evolution-on-a-chip. *Trends in Biotechnology.* **40** (1), 60-76 (2022).
33. Kamalinia, G., Grindel, B. J., Takahashi, T. T., Millward, S. W., Roberts, R. W. Directing evolution of novel ligands by mRNA display. *Chemical Society Reviews.* **50** (16), 9055-9103 (2021).
34. Godino, E. et al. De novo synthesized Min proteins drive oscillatory liposome deformation and regulate FtsA-FtsZ cytoskeletal patterns. *Nature Communications.* **10**, 4969 (2019).
35. Tenchov, R., Bird, R., Curtze, A. E., Zhou, Q. Lipid nanoparticles─From liposomes to mRNA vaccine delivery, a landscape of research diversity and advancement. *ACS Nano.* **15** (11), 16982-17015 (2021).
36. Deshpande, S., Caspi, Y., Meijering, A. E., Dekker, C. Octanol-assisted liposome assembly on chip. *Nature Communications.* **7**, 10447 (2016).
37. Schaich, M. et al. An integrated microfluidic platform for quantifying drug permeation across biomimetic vesicle membranes. *Molecular Pharmaceutics.* **16** (6), 2494-2501 (2019).

38. Schaich, M., Sobota, D., Sleath, H., Cama, J., Keyser, U. F. Characterization of lipid composition and diffusivity in OLA generated vesicles. *Biochimica et Biophysica Acta (BBA)-Biomembranes.* **1862** (9), 183359 (2020).

39. Deshpande, S., Spoelstra, W. K., Van Doorn, M., Kerssemakers, J., Dekker, C. Mechanical division of cell-sized liposomes. *ACS Nano.* **12** (3), 2560-2568 (2018).

40. Juskóva, P. et al. "Basicles": Microbial growth and production monitoring in giant lipid vesicles. *ACS Applied Materials & Interfaces.* **11** (38), 34698-34706 (2019).

41. Fletcher, M. et al. DNA-based optical quantification of ion transport across giant vesicles. *ACS Nano.* **16** (10), 17128-17138 (2022).

42. Vaezi, Z. et al. Investigation of the programmed cell death by encapsulated cytoskeleton drug liposomes using a microfluidic platform. *Microfluidics and Nanofluidics.* **24** (7), 48 (2020).

43. Al Nahas, K. et al. A microfluidic platform for the characterisation of membrane active antimicrobials. *Lab on a Chip.* **19** (5), 837-844 (2019).

44. Bao, P. et al. Production of giant unilamellar vesicles and encapsulation of lyotropic nematic liquid crystals. *Soft Matter.* **17** (8), 2234-2241 (2021).

45. Yandrapalli, N., Petit, J., Bäumchen, O., Robinson, T. Surfactant-free production of biomimetic giant unilamellar vesicles using PDMS-based microfluidics. *Communications Chemistry.* **4**, 100 (2021).

46. Cama, J. et al. An ultrasensitive microfluidic approach reveals correlations between the physico-chemical and biological activity of experimental peptide antibiotics. *Scientific Reports.* **12**, 4005 (2022).

47. Guerzoni, L. P. et al. High macromolecular crowding in liposomes from microfluidics. *Advanced Science.* **9** (27), e2201169 (2022).

48. Gonzales, D. T., Yandrapalli, N., Robinson, T., Zechner, C., Tang, T. D. Cell-free gene expression dynamics in synthetic cell populations. *ACS Synthetic Biology.* **11** (1), 205-215 (2022).

49. Ushiyama, R., Koiwai, K., Suzuki, H. Plug-and-play microfluidic production of monodisperse giant unilamellar vesicles using droplet transfer across water-oil interface. *Sensors and Actuators B: Chemical.* **355**, 131281 (2022).

50. Banlaki, I., Lehr, F.-X., Niederholtmeyer, H. Microfluidic production of porous polymer cell-mimics capable of gene expression. In *Cell-Free Gene Expression.*, edited by Karim, A. S., Jewett, M. C., 237-255. Humana. New York, NY (2022).